

Computational Rutherford Experiment Utilizing Monte Carlo Sampling

Chance Jackson* and Nico O'Neill†
Syracuse University Department of Physics
(Dated: October 22, 2025)

In this work, we utilized Monte Carlo methods and numerical integration techniques to verify the expected relationships between various scattering parameters and the scattering angle as predicted by the theory of Rutherford scattering, the elastic scattering of charged particles due to the Coulomb interaction [1]. We correctly observed that the cotangent of the scattering angle depended linearly on the incident energy of the scattered particle, and was inversely proportional to the atomic number of the target nuclei. Finally, we comment on the computational complexity of our algorithm, noting that the time complexity appears to scale linearly with the number of simulated particles.

1. INTRODUCTION

1.1. Rutherford's Experiment

The Rutherford Scattering experiments were conducted in 1906 and were used to prove the Rutherford model of the atom. The experiment was conducted by firing an alpha particle beam at a thin metal foil. If the previous model of the atom, the Thomson model, was correct, we could expect the alpha particle to transmit fully through the foil. Rather, Rutherford and his team saw some of the alpha particles scatter in various directions, meaning they needed to be repelled by something. This confirmed a new model of the atom, one with a massive nucleus surrounded by positive charge[2].

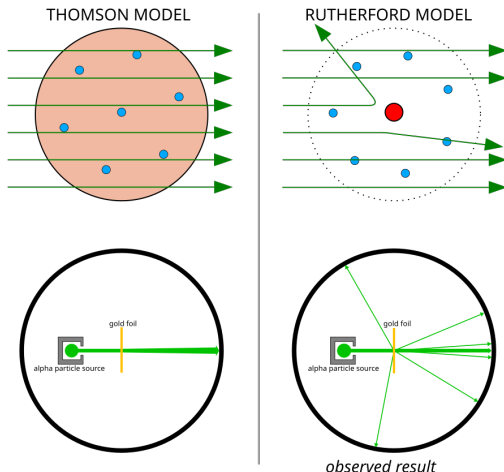


FIG. 1: A depiction of the varying expected results of the Rutherford experiment.

The fundamental cause of the experimental outcome is the Coulomb interaction between the alpha particle and one of the foil nuclei.

For an alpha particle with charge Z_1 scattering from a nucleus of charge Z_2 , the interaction is governed by the Coulomb force:

$$\mathbf{F}(\mathbf{r}) = \frac{kZ_1Z_2}{r^2} \hat{\mathbf{r}}. \quad (1)$$

where k is the Coulomb constant.

1.2. Monte Carlo Methods

Monte Carlo methods refers to a broad class of algorithms which, at their core, utilize random sampling to numerically solve problems. There are numerous applications of these techniques, including as powerful numerical integrators, where their unique uncertainty scaling (which is independent of the dimensionality of the function being integrated) leads to them potentially outperforming deterministic methods in certain cases [3]. In our work, we exploit a different application of Monte Carlo methods: as a tool to model random processes by drawing samples from probability distributions. In their original work, Rutherford and his team used various radioactive sources to produce the alpha particles which they scattered off of their gold foil. Given that nuclear decay is a random process (and hence, governed by probability distributions), in order for us to accurately model it will require us to incorporate an element of randomness into our simulation, which is possible through Monte Carlo methods.

2. SIMULATION

Broadly, our simulation proceeds in three steps: sample the energy distribution to determine the incident energy (in other words, the initial energy) of the scattered alpha particle, sample the impact parameter distribution to determine the impact parameter (the initial perpendicular distance between the scattered alpha particle and the target nuclei) of the scattered alpha particle, and evolve the trajectory of the scattered alpha particle according to the Coulomb interaction between it and the target nuclei. The specifics of each of these three steps are explored in the following section.

*Electronic address: cjacks34@syr.edu

†Electronic address: neoneill@syr.edu

2.1. Sampling Distribution Functions

In order to allow for randomness in both the incident energy and impact parameter of our scattered particles, our Monte Carlo simulation relied on samples drawn from two distributions: a power-law and a Gaussian. We used the Gaussian to model the energy distribution of emitted alpha particles from a radioactive source, and the power-law to model the impact parameter.

We defined our power-law probability density function as:

$$PDF(x) = ax^{a-1}; \quad a > 0, \quad x \in (0, 1], \quad (2)$$

with a a constant which determines the shape of our power-law. In our case, we used $a = 0.5$, meaning our power-law followed an inverse square root. Likewise, we defined our Gaussian distribution in the standard way:

$$PDF(x) = \frac{1}{\sqrt{2\pi\sigma^2}} e^{-\frac{(x-\mu)^2}{2\sigma^2}}, \quad (3)$$

with μ the mean of the distribution and σ the standard deviation.

To generate samples from these distributions, we used both rejection sampling and the Inverse CDF method. Since there is no closed form integral of the Gaussian function in terms of elementary functions, we elected to sample from the Gaussian distribution using rejection sampling. This simple procedure involved uniformly sampling points on a two-dimensional grid, and only accepting those which are below the curve of our Gaussian distribution. These accepted samples will follow a Gaussian distribution. A drawback of this method is that, depending upon the parameters of the Gaussian in question, it can take many random samples until one is accepted, so generating large sets of accepted samples can be computationally prohibitive. In contrast, the Inverse CDF method randomly samples the inverse of the cumulative density function (CDF) (the integral of the PDF), which produces samples distributed according to the PDF. Since our power-law PDF is easily integrated, we used this method to draw samples from it.

2.2. Interparticle Interaction Modeling

The interaction between the alpha particle and the nucleus of the foil is calculated using the Coulomb force, as shown in Eq. 1. This force is used to calculate acceleration via Newton's law, and the state is updated through the Runge-Kutta 4 integration method.

Our Coulomb force calculation is of time and space complexity $O(1)$, as it simply performs operations on a vector. The update step is of time and space complexity $O(N)$, as it loops an $O(1)$ complexity step N times. This makes the expected overall complexity of our code $O(N)$. We do expect to see errors arising from this section of

code. It utilizes high-precision numbers, such as the elementary charge, which will lead to rounding errors. From the use of RK4, we expect to see numerical integration errors, which may appear as a loss of energy conservation over time.

3. RESULTS AND VALIDATION

3.1. Standard Rutherford Scattering

The first test we ran was a simple verification of whether our simulation was scattering using fixed input parameters. We set a gold nucleus at the origin and fired 3 alpha particles at it with varying impact parameters.

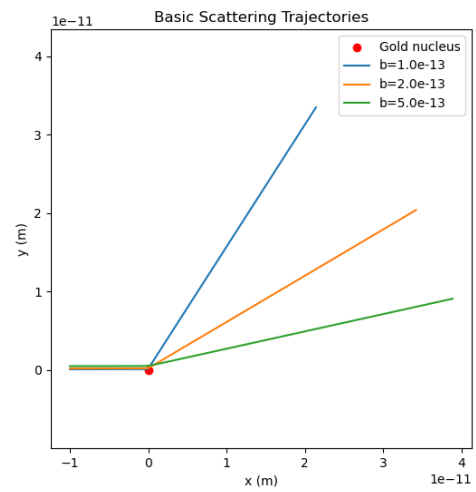


FIG. 2: A simulation of Rutherford scattering with varying impact parameters.

Qualitatively, we see that this result fits our expectation. We see that as the alpha particles reach the nucleus, they scatter at varying angles. As seen in Fig. 1, our particles were similarly scattered away as we expected them to. The relationship between the impact parameter and the scattering angle is discussed later.

3.2. Power-Law Scattering

Our next experiment incorporates a Monte Carlo simulated power-law distribution. We used this distribution to randomly sample and collect the impact parameters of particles that would interact with the nucleus and plotted 100 of those results.

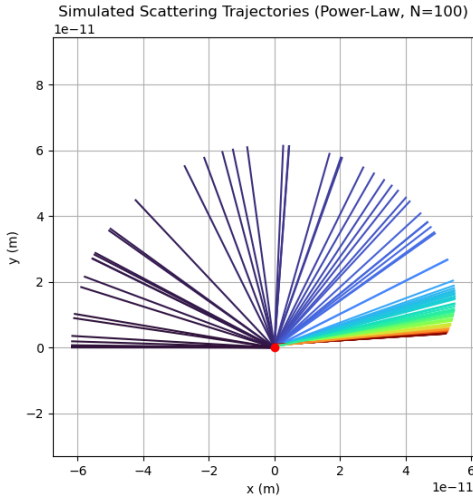


FIG. 3: A simulation of Rutherford scattering with impact parameters chosen through Monte Carlo sampling.

Once again, we see the scattering effect we want. With this color map, the darker blue colors represent smaller impact parameters, while the red represents larger impact parameters. From this plot, we can see that our angles decrease as b increases, or in other words, for the bluer lines, we see higher deflection. Theoretically, the relationship between the impact parameter and the scattering angle is:

$$\theta = 2 \arctan \left(\frac{k Z_1 Z_2}{2bE} \right)$$

$$\tan \left(\frac{\theta}{2} \right) = \frac{k Z_1 Z_2}{2bE}$$
(4)

where we can see that the impact parameter, b , and the incident energy, E , are both inversely proportional to the tangent of half the scattering angle [4].

3.3. Scattering Angle Distribution

We produced histograms of the scattering angles for the power-law distribution impact parameters to see how the distribution changes. From experimentation, we expect to see a large peak at $\theta = 0$. This is because most particles do have a large b , meaning that they mostly pass by the nucleus and only feel a small deflection effect. Experimental results showed the following distribution.

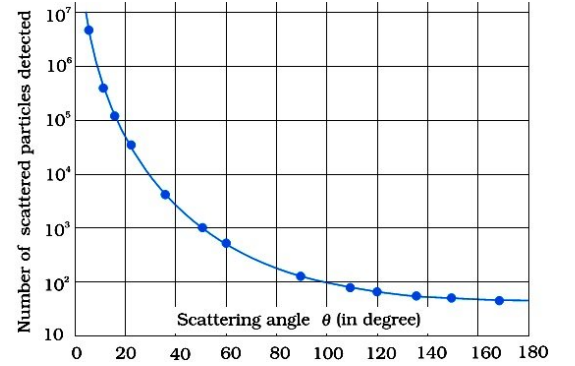


FIG. 4: An experimental result from the Rutherford Scattering experiment.[5]

We plotted ours for 3 different sample sizes, and allowed for positive and negative b , meaning we expected to see a symmetric plot (due to the angular symmetry of our problem) peaking around 0.

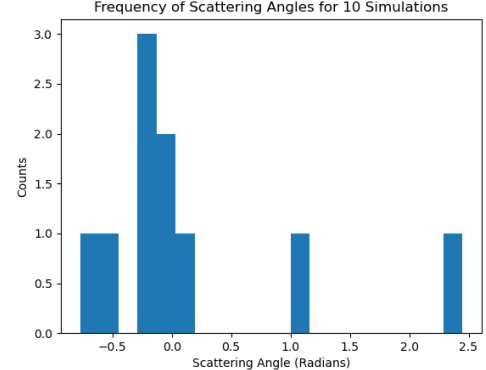


FIG. 5: A histogram of the scattering angle with sample size 10.

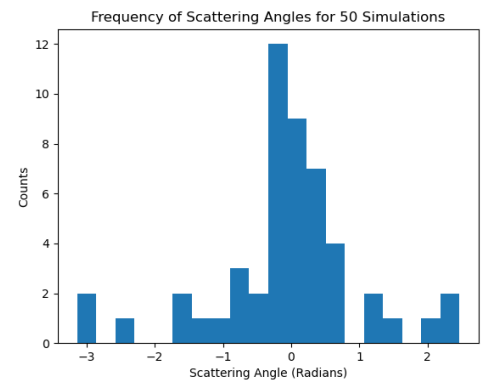


FIG. 6: A histogram of the scattering angle with sample size 50.

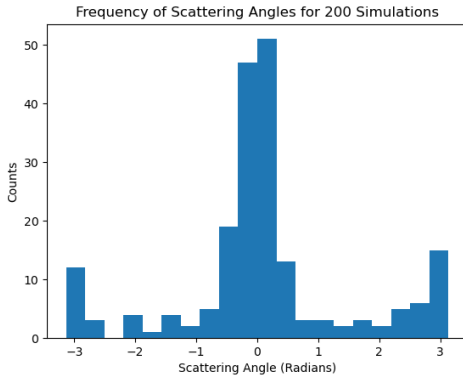


FIG. 7: A histogram of the scattering angle with sample size 200.

As expected, we see a concentration of points about $\theta = 0$, with the larger sample size of data becoming more accurate.

3.4. Effect of Incident Energy on Scattering Angle

With the impact parameter fixed, we drew incident energy samples randomly from the Gaussian distribution described in Sec. 2.1. Figure 8 shows these energies plotted against the scattering angle of the scattered alpha particle. We observed that the incident energy appears to be directly proportional to the cotangent of half the scattering angle, exactly the relation which appears in Eq. 4.

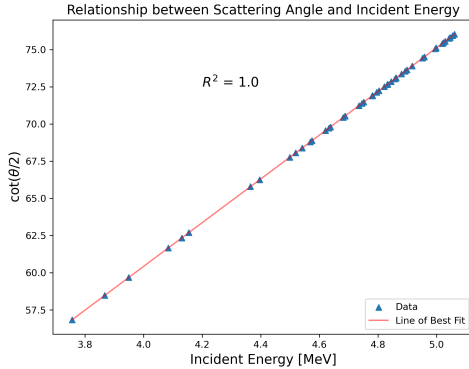


FIG. 8: Simulated relationship between incident energy and scattering angle (θ). We observed the relation described in Eq. 4, since it's clear from this plot that $E \propto \cot(\frac{\theta}{2})$, confirmed by the high Coefficient of Determination.

3.5. The Effect of Scattering Nuclei on Scattering Angle

With both the impact parameter and the incident energy fixed, we varied the atomic number of the target

nuclei and observed the change in the scattering angle. Figure 9 shows a plot of this data, from which its clear that the atomic number is directly proportional to the tangent of half the scattering angle, again confirming the relation laid out in Eq. 4.

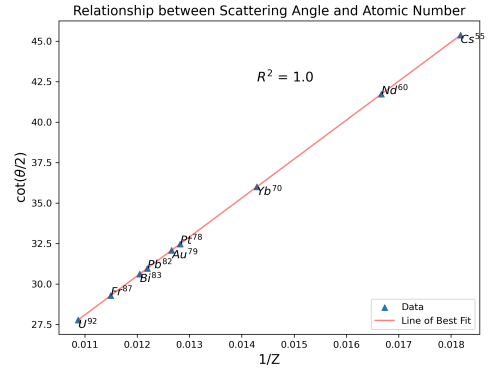


FIG. 9: Simulated relationship between atomic number of target nuclei and scattering angle. The high Coefficient of Determination confirms that $Z \propto \tan(\frac{\theta}{2})$, as expected from Eq. 4.

3.6. Time Complexity

By measuring the time it takes for our simulation codes to run, we were able to assess the time complexity of our algorithm. Figure 10 shows the fraction of the total runtime that each individual simulation step takes, from which its clear that our largest bottleneck occurs during the numerical integration of the scattered particle's trajectory. This means that the time complexity of our algorithm is simply the time complexity of our trajectory update step, to good approximation. As mentioned in Sec. 2.2, we expect the time complexity of the update step to be $O(N)$, with N the number of particles being simulated. To validate this, we measured the total time taken for our simulation to run for different numbers of particles, the result of which is shown in Fig. 11.

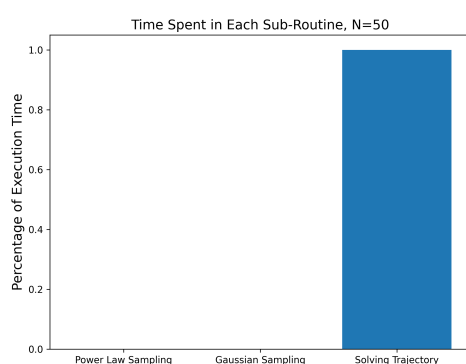


FIG. 10: A plot of where time is being taken up during a simulation run.

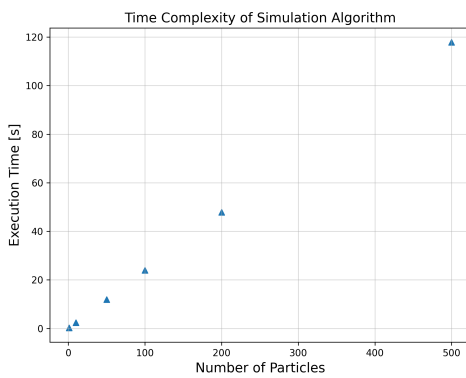


FIG. 11: A model showing the $O(N)$ complexity of the code.

Since we do observe the anticipated linear relation between particle number and execution time, our plots show that we accurately calculated our time complexity.

4. CONCLUSIONS

We were able to use Monte Carlo methods and numerical integration techniques to replicate the results of the famous Rutherford scattering experiments. We observed the correct relationships between different scattering parameters and the scattering angle, validating our method. Finally, we demonstrated that our algorithm does exhibit the time complexity we would expect from a first-principles analysis of our code.

-
- [1] Physik-Institut and I. Neutelings, Tech. Rep. (2017), URL https://indico.cern.ch/event/1126814/contributions/4729554/attachments/2386887/4079372/Izaak_paper_reading_Rutherford_nucleus_20170713_v5.pdf.
 - [2] E. Rutherford, *The Structure of the Atom* (1914), URL <https://www.chemteam.info/Chem-History/Rutherford-1914.html>.
 - [3] M. E. J. Newman, *Computational Physics* (Createspace Independent Publishing Platform, 2013).
 - [4] Wikipedia, *Rutherford scattering experiments* (2025), URL https://en.wikipedia.org/wiki/Rutherford_scattering_experiments.
 - [5] P. O. Lab, *The Rutherford-Geiger-Marsden Experiment* (2017), URL <https://physicsopenlab.org/2017/04/11/the-rutherford-geiger-marsden-experiment/>.